

Cite this: *Mater. Adv.*, 2026,  
7, 241

## Recycling PVC waste into a functional adsorbent for dye removal: an eco-friendly approach

Lokman Hosen,<sup>a</sup> Md Abdul Goni,<sup>\*b</sup> Most. Johura Khatun<sup>a</sup> and  
Sharmeen Nishat<sup>ib</sup><sup>\*a</sup>

Environmental pollution caused by the improper discharge of toxic dyes from industries has become a major concern nowadays in developing countries. A facile route was explored to develop a new cost-effective, modified waste material-based adsorbent. Plastic solid wastes, such as waste PVC pipes, were processed and converted into a functional material, which was applied in dye removal technology. PVC was separated from the plastic waste with an extraction yield of 78%. The isolated PVC was modified functionally by treating it with ethylenediamine. Characterization of the product by elemental analysis, XPS, and FT-IR techniques confirmed the formation of aminated PVC (APVC). A series of adsorption batch experiments were carried out by APVC to remove methylene blue (MB) dye from solutions. The MB removal efficiency was optimized by varying different experimental parameters including solution pH, contact time, dye concentration, adsorbent dose, and temperature. An adsorption capacity of 10.45 mg g<sup>-1</sup> with 52.25% of MB removal was recorded under optimized conditions (pH 10, contact time of 11 hours, dye concentration of 20 ppm, adsorbent dose of 10 mg/10 mL, and temperature of 30 °C). The experimental data best fitted with the Langmuir isotherm ( $R^2 = 0.9699$ ) and followed pseudo second-order kinetics ( $R^2 = 0.9914$ ). Evaluation of different thermodynamic parameters (negative  $\Delta G^\circ$ ,  $\Delta H^\circ = 9.7524$  kJ mol<sup>-1</sup>, and  $\Delta S^\circ = 33.5474$  J K<sup>-1</sup> mol<sup>-1</sup>) demonstrated the spontaneous and endothermic nature of the MB adsorption process on APVC. These results reveal a new avenue for plastic solid waste management by recycling and modifying PVC waste into valuable functional materials that work as potential adsorbents for the efficient removal of dyes from wastewater systems.

Received 28th April 2025,  
Accepted 29th October 2025

DOI: 10.1039/d5ma00411j

rsc.li/materials-advances

### 1. Introduction

Water has long been recognized as an essential component for the survival and continuation of life throughout the biosphere. However, human activities, application of radioactive isotopes, oil spills, industrial effluents, and agricultural runoffs are constantly polluting different natural water resources.<sup>1–3</sup> The discharge of wastewater from different sources, particularly from various industries and urban activities, without any prior treatment or with partial treatment has become a major concern nowadays in many developing countries since they contain different toxic contaminants, which severely impact the terrestrial environment and the health of millions of people.<sup>4</sup> The rapid growth of industrialization worldwide causes the continuous increase in wastewater discharge, which has a detrimental effect on aquatic ecology. Dyes are the most common organic contaminants, which are released as toxic mixed wastewater

from different industries in Bangladesh. The presence of toxic dyes in water bodies could drastically modify the photosynthetic processes of marine biological cycles. Most dye species are not biodegradable, and they are known to cause allergies and cancer and induce mutations. Additionally, dyes may induce failure of the kidneys, liver, brain, and lungs and can cause nervous system issues if they are ingested in the human body with water or other sources.<sup>5–10</sup> Hence, the presence of toxic dyes in effluents is a matter of serious concern because of their harmful impacts on both humans and the terrestrial environment. Even at very low concentrations, the hues of these dyes are immediately identifiable, which make them very conspicuous and undesirable in the respective environmental components.<sup>11,12</sup> Nowadays, different types of dyes are used in the textile, leather, and painting industries. Methylene blue is a synthetic cationic basic dye used to colour cotton, silk, wool, and leather. It is also utilized to coat paper stock and in labs for electrophoresis, blotting, DNA extraction, and RNA extraction. Methylene blue (MB), also known as tetramethyl thionine chloride, possess the molecular structure of a heterocyclic aromatic compound.<sup>13</sup> It has been recognized as a popular dye due to its worldwide application in different industries

<sup>a</sup> Department of Chemistry, Bangladesh University of Engineering and Technology, Dhaka-1000, Bangladesh. E-mail: snnupur@chem.buet.ac.bd

<sup>b</sup> Department of Biological and Physical Sciences, South Carolina State University, Orangeburg, SC 29117, USA



such as textile, paper, rubber, plastics, leather, cosmetics, pharmaceutical, and food processing. These industries discharge very large volumes of dyes continuously as mixed effluents into the surrounding waterbodies and lands, which pose a serious threat to the terrestrial environment. However, although many industries have tried to treat effluents prior to their discharge, analysis of wastewater released from these industries showed the presence of significant quantities of dye residues.<sup>14,15</sup> Therefore, it is highly necessary to utilize suitable technology that can effectively extract and remove toxic pollutants from industrial waste streams, and thus reduce the pollution in natural waterbodies, land and other environmental segments.<sup>16</sup> Phase-change technologies known as adsorption processes have gained popularity in recent years because of their ease of use, comparative affordability and high effectiveness in removing pollutants from aqueous solutions even at low concentrations.<sup>17,18</sup> Polyvinyl chloride (PVC) is a versatile thermoplastic widely utilized, with its demand reaching 35 million tons annually on a global scale.<sup>19</sup> Because of its many advantages and diverse qualities such as chemical stability, corrosion resistance, low cost,<sup>20–22</sup> and especially ease of processing, as well as its important compatibility with different additives,<sup>23</sup> PVC has emerged as the most widely utilized material nowadays.<sup>24–26</sup> A wide variety of products has been manufactured using PVC as the principal raw material, which include window frames, drainage pipes, water service pipes, medical devices, blood storage bags, cable and wire insulation, resilient flooring, roofing membranes, stationary, automotive interiors and seat coverings, fashion and footwear, and packaging.<sup>27,28</sup> These large varieties of PVC products ultimately generate an extensive quantity of solid waste after their use in different sectors (approximately 5.5 million tons of PVC waste is generated globally each year). Unfortunately, the waste generated from different PVC products is not biodegradable, and thus causes severe pollution in the terrestrial environment. Accordingly, several methods for PVC recycling have been reported in the literature.<sup>29–33</sup> However, most of these PVC recycling methods have been found to be ineffective and not viable for practical applications because of the formation of a high percentage of chlorine as byproduct.<sup>29</sup> Particularly, the unidentified risks associated with the oxidative decomposition of PVC in the environment by landfilling and composting of PVC products without any processing are noticeable.<sup>30,31</sup> Also, due to the generation of substantial volumes of hydrogen chloride and other hazardous by-products, the incineration and pyrolysis of PVC waste are strongly discouraged in many countries as these methods pose a significant threat to the environment and human health.<sup>29,32,33</sup> Therefore, it is highly necessary to introduce and develop potential approaches to effectively manage plastic waste and minimize the environmental pollution from PVC waste. However, limited data are available on the conversion of PVC waste into useful products that can remove toxic pollutants from wastewater bodies. The removal of ions by modified waste PVC was reported previously in the literature.<sup>34</sup> Several studies reported dye removal processes using modified PVC.<sup>35,36</sup> These studies used virgin PVC and modified it for its

application in dye removal processes. However, to the best of our knowledge, no study has been carried out on dye removal technology utilizing waste PVC products to date. Also, no data are available in the literature on the potential removal of dyes from aqueous solutions using functionalized materials synthesized from waste PVC products. The present study aimed to convert plastic solid waste into functional materials and apply the resulting materials in dye removal technology. It focused on the synthesis and characterization of amino functional PVC materials by utilizing solid plastic waste products and finding potential applications of modified functionalized PVC materials as effective adsorbents in the removal of dyes from wastewater using adsorption technology. Therefore, the novelty and significance of the present study lie in its ability to address two environmental issues simultaneously, *i.e.*, plastic waste reuse and water pollution remediation, by integrating waste management with water treatment technologies.

## 2. Materials and methods

### 2.1 Materials

All the materials used in this research were of analytical grade. Tetrahydrofuran (THF) anhydrous was purchased from Sigma-Aldrich (USA) with 99.9% purity. Ethylenediamine ( $C_2H_8N_2$ ,  $\geq 99\%$ ), pyridine, sodium hydroxide ( $NaOH$ ,  $\geq 98\%$ ), sulphuric acid ( $H_2SO_4$ , 98%), and methylene blue were obtained from Merck Millipore (Merck KGaA, Darmstadt, Germany).

### 2.2 Methodology

#### 2.2.1 Extraction of PVC polymer from plastic solid waste.

Several methods have been reported in the literature to extract and separate PVC polymer from solid plastic waste.<sup>37,38</sup> In the present study, waste PVC pipe was utilized to extract and isolate the PVC polymer following a standard technique.<sup>38</sup> The solvent extraction method was used to isolate PVC polymer from plastic solid waste. Additive-free pure PVC was extracted and separated from plastic solid waste by using an organic solvent. Fig. 1 shows the different steps of extraction and separation of PVC polymer from waste PVC pipes.

#### 2.2.2 Structural modification of extracted PVC.

Extracted PVC was modified by the introduction of amino functionality. In this study, isolated PVC was chemically treated with ethylene diamine solution following a standard procedure.<sup>39,40</sup> During the experimental process, 10 g  $\approx$  11 mL ethylenediamine (EDA) solution was added dropwise to 1 g of polyvinyl chloride (PVC) in a 100 mL round-bottom flask.<sup>39</sup> The mixture was vigorously

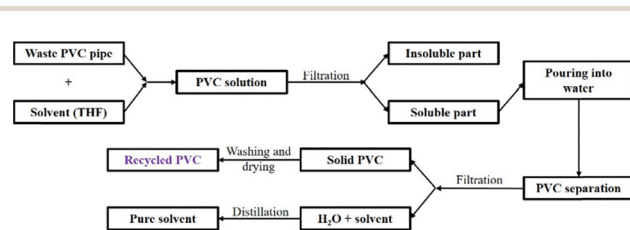


Fig. 1 PVC extraction process.



stirred in an oil bath at room temperature for 4 h under a nitrogen atmosphere. After completion of the reaction, the resulting mixture was filtered and the solid aminated PVC product was deposited on filter paper, which was washed thoroughly with DI water to eliminate the unreacted EDA and other by-products (HCl and EDA·HCl). Finally, the aminated PVC was dried for two days in an oven at 45 °C. The desired product was analysed by FT-IR and other standard techniques.

**2.2.3 Batch adsorption experiments.** A series of batch experiments was carried out utilizing the functionalized extracted PVC as a potential adsorbent. All adsorption experiments were conducted following the standard procedures and different factors such as effects of temperature, adsorbent dose, contact time, pH, and initial dye concentration were studied during the batch experiments.

A stock solution of methylene blue (MB) with a concentration of 100 ppm was made accordingly, which was used in the batch experiments. This stock solution (100 ppm) was utilized to prepare 5, 10, 15, 20, and 25 mg L<sup>-1</sup> solution of MB by using standard dilution procedures and the pH of each MB solution with a particular concentration was maintained at 10.

**2.2.3.1 Optimization of pH in analyte solutions.** The adsorption experiments were carried out by varying the pH in the range of 2 to 10 to investigate the impact of pH on the removal of methylene blue (MB) from aqueous solutions. The pH of the MB solutions was adjusted using 0.01 M NaOH and 0.01 M H<sub>2</sub>SO<sub>4</sub> solutions. Given that PVC and HCl both contain chloride ions, HCl was not employed to adjust the pH of the respective solutions to prevent a possible common ion effect. In the experimental processes, 10 mL of dye solution with a fixed initial concentration of 20 mg L<sup>-1</sup> was taken in a stoppered conical flask. 10 mg of modified PVC (MPVC) was added, and the resulting mixture was agitated in a shaker for 12 h at a speed of 180 rpm.

**2.2.3.2 Optimization of initial analyte concentration.** In this study, 10 mL of dye solution at various starting concentrations of 5, 10, 15, 20, and 25 mg L<sup>-1</sup> was used. In each case, 10 mL of MB solution with a pH of 10 was added to a fixed amount (10 mg) of MPVC in a conical flask equipped with a stopper and the resulting mixture was stirred in a shaker at a constant agitation speed of 180 rpm for 12 h.

**2.2.3.4 Adsorbent dose optimization.** In this study, different amounts of MPVC such as 5, 10, 15, 20, and 25 mg were separately added to 10 mL of MB solution at pH 10 in 250 mL stoppered glass Erlenmeyer flasks. The resulting mixtures in the Erlenmeyer flasks were agitated on an orbital shaker at 170 rpm for 16 h. The mixtures were filtered using Whatman 41 filter paper and the resulting filtrate was analysed by using a UV-vis spectrophotometer (Shimadzu Model UV-1800, Japan) at the maximum wavelength of 663 nm. Thus, the concentration of MB in the respective aqueous solutions was determined before and after the adsorption experiments. Eqn (1) and (2) were used to determine the adsorption capacity ( $q_e$ ) and percent

adsorption of the dye from aqueous solutions, respectively.<sup>41</sup>

$$q_e = \frac{(C_i - C_e)V}{W} \quad (1)$$

$$\% \text{removal} = \frac{C_i - C_e}{C_i} \times 100 \quad (2)$$

where  $C_i$  represents the initial concentration of MB in aqueous solution in mg L<sup>-1</sup> and  $C_e$  represents the concentration of MB in mg L<sup>-1</sup> at equilibrium condition.  $V$  represents the volume of the experimental solution (in L) and  $W$  is the mass of MPVC (in g) used in the corresponding adsorption experiments.

#### 2.2.4 Statistical analysis

**2.2.4.1 Isotherm modelling.** Different thermodynamic models such as Langmuir, Freundlich, and Temkin isotherm models were utilized to investigate and evaluate the adsorption characteristics of methylene blue dye on the surface of MPVC.

**2.2.4.1.1 Langmuir isotherm.** The Langmuir isotherm model considers the adsorbent surface as a monomolecular layer combination with no intermolecular interactions, where potential active sites are available to bind analyte molecules. Eqn (3) represents the Langmuir isotherm model in linear form. In this equation,  $q_e$  denotes the amount of dye adsorbed on the solid surface (mg g<sup>-1</sup>),  $C_e$  is the equilibrium adsorbate concentration (mg L<sup>-1</sup>), and  $q_{\max}$  and  $K_L$  represent the Langmuir constants, which correspond to the maximum adsorption capacity (mg g<sup>-1</sup>) and energy of adsorption (L mol<sup>-1</sup>), respectively. A dimensionless component,  $R_L$ , is identified as the major feature of the Langmuir isotherm, which is described as follows:

$$R_L = \frac{1}{1 + K_L C_0}$$

The magnitude of  $R_L$  indicates the type and nature of adsorption, which can be categorized as unfavourable ( $R_L > 1$ ), linear ( $R_L = 1$ ), favourable ( $0 < R_L < 1$ ), or irreversible ( $R_L = 0$ ).<sup>42</sup>

$$\frac{1}{q_e} = \frac{1}{K_L q_{\max}} \times \frac{1}{C_e} + \frac{1}{q_{\max}} \quad (3)$$

**2.2.4.1.2 Freundlich isotherm.** The Freundlich isotherm model predicts the multilayer adsorption process on a solid adsorbent as well as the heterogeneous surface characteristics of the corresponding adsorbent material. This isotherm model can also be utilized to determine the sorption energy and assess the interactions between the molecules adsorbed on solid surfaces. The empirical Freundlich isotherm model can be quantitatively expressed in the form of eqn (4), which can be utilized to characterize the heterogeneous characteristics of dye adsorption on solid surfaces. The Freundlich parameters  $K_f$  (mg<sup>(1-n)</sup> L<sup>n</sup> g<sup>-1</sup>) and  $1/n$  indicate the adsorption capacity and adsorption strength of solid materials, respectively.<sup>43-45</sup> The magnitude of  $n$  can be utilized to predict whether the corresponding adsorption of metals or dyes on solid adsorbents occurs *via* chemisorption or physisorption processes. If the value of  $n$  is less than 1, the sorption process is considered



chemisorption. However, if the magnitude of  $n$  is observed to be higher than 1, the sorption process is assumed to proceed *via* the physisorption mechanism.<sup>46</sup>

$$\log q_e = \frac{1}{n} \log C_e + \log K_f \quad (4)$$

**2.2.4.1.3 Temkin isotherm.** The generic Temkin isotherm model was built on the premise that the heat of adsorption would decrease linearly and that the binding energies would be distributed uniformly up to a maximum value. The Temkin isotherm can be expressed in the form of eqn (5). In this equation,  $A_T$  denotes the equilibrium binding constant corresponding to the maximum binding energy, the constant  $RT/b_T$  indicates the heat of adsorption,  $R$  is the universal gas constant,  $T$  is the absolute temperature in Kelvin and  $1/b_T$  represents the adsorption potential of the adsorbent. All these parameters can be determined from the plot of  $\ln C_e$  versus  $q_e$  following eqn (5).<sup>46</sup>

$$q_e = \frac{RT}{b_T} \ln A_T + \frac{RT}{b_T} \ln C_e \quad (5)$$

**2.2.4.2 Thermodynamic parameters.** Different thermodynamic parameters such as  $\Delta G^\circ$ ,  $\Delta S^\circ$  and  $\Delta H^\circ$  associated with the dye adsorption on MPVC were assessed following the standard procedures.<sup>47,48</sup> The following characteristic equations were used to calculate the standard free energy ( $\Delta G^\circ$ , kJ mol<sup>-1</sup>), standard enthalpy ( $\Delta H^\circ$ , kJ mol<sup>-1</sup>), and standard entropy ( $\Delta S^\circ$ , J mol<sup>-1</sup> K<sup>-1</sup>) of the dye adsorption process.<sup>43,44</sup>

$$\Delta G^\circ = -RT \ln K_L \quad (6)$$

$$\Delta G^\circ = \Delta H^\circ - T\Delta S^\circ \quad (7)$$

$$\ln K_L = -\frac{\Delta H^\circ}{RT} + \frac{\Delta S^\circ}{R} \quad (8)$$

where  $R$  denotes the universal gas constant (8.314 kJ mol<sup>-1</sup> K<sup>-1</sup>),  $K_L$  represents the Langmuir equilibrium constant (L mol<sup>-1</sup>),  $T$  is the absolute temperature (K),  $q_e$  represents the adsorption capacity and  $C_e$  is the equilibrium dye concentration. The plot of  $\ln K_L$  vs.  $1/T$  yields a straight line, where the slope and intercept of the straight line reveal the changes in enthalpy ( $\Delta H^\circ$ ) and entropy ( $\Delta S^\circ$ ) associated with the removal of MB dye from aqueous solutions by MPVC, respectively. The magnitude of  $K_L$  can be determined by using eqn (9), as follows:<sup>45</sup>

$$K_L = \frac{q_e}{C_e} \quad (9)$$

**2.2.4.3 Kinetic modelling study.** Kinetic investigation provides significant information on the type of adsorption and the possible mechanism of the corresponding process occurring in the removal of dye by solid adsorbents.<sup>45</sup> The adsorption kinetics is assumed to proceed *via* four sequential steps, as follows: (1) the water layer on the hydrated adsorbent surface allows the adsorbate species to diffuse from the bulk solution

to the surface, (2) the adsorbate overcomes the resistance of the liquid film on the adsorbent surface, (3) the adsorbate species diffuse from the exterior surfaces and reach to inner surface active sites of the adsorbent and (4) the adsorbate species and the active sites on the surface of the adsorbent interact with each other.<sup>49</sup> The adsorption kinetics associated with the removal of MB dye from aqueous solution by MPVC were investigated and evaluated by inputting the experimental data in the pseudo-first-order, and pseudo-second-order kinetic model equations.<sup>45,50</sup>

**2.2.4.3.1 Pseudo-first-order kinetic model.** Lagergren's first-order rate equation was used to express the dye adsorption rate on the surface of MPVC, which was calculated based on the degree of adsorption. The linear version of Lagergren's first-order rate equation can be written as follows:<sup>1,51,52</sup>

$$\ln(q_e - q_t) = \ln q_e - K_1 t \quad (10)$$

where  $q_e$  (mg g<sup>-1</sup>) denotes the equilibrium amount of dye adsorbed on the biosorbent material,  $q_t$  (mg g<sup>-1</sup>) is the amount of dye adsorbed on the surface of the biosorbent at any given moment, and  $K_1$  (min<sup>-1</sup>) is the rate constant of the pseudo-first-order adsorption, which is determined from the slope of the linear equation obtained from the plot of  $\ln(q_e - q_t)$  vs.  $t$  (slope =  $K_1$ ,  $q_e$  = experimental intercept).

**2.2.4.3.2 Pseudo-second-order kinetic model.** Ho introduced a second-order reaction model for the biosorption of dissociated metals ions in charcoal particles based on the adsorption capacity of biosorbents. The solvent composition in the analyte solution could change the dynamics of the second-order rate, where biomass and other solutes solutions could show pseudo-second-order reaction kinetics. The mathematical expression for the pseudo-second-order kinetic model was introduced and reported by Ho, which is displayed as eqn (11), as follows:<sup>1,42,45,51,53,54</sup>

$$\frac{t}{q_t} = \frac{1}{k_2 q_e^2} + \frac{t}{q_e} \quad (11)$$

where  $q_e$  represents the quantity of dye adsorbed at equilibrium on the surface of the biosorbent (mg g<sup>-1</sup>),  $q_t$  is the amount of dye (mg g<sup>-1</sup>) adsorbed at any time  $t$  during the biosorption process biosorbent, and  $K_2$  (g mg<sup>-1</sup> min<sup>-1</sup>) refers to the adsorption rate constant of the pseudo-second-order reaction. The magnitude of  $K_2$  (g mg<sup>-1</sup> min<sup>-1</sup>) can be determined from the slope and intercept of the equation obtained from the plot of  $t/q_t$  versus  $t$ .

## 3. Results and discussion

### 3.1 Extraction of PVC from solid waste and modification of extracted PVC

Solid PVC pipe waste was processed, and the solvent extraction method was utilized to extract and separate PVC polymer from the waste products. Application of THF in the extraction procedures yielded about 78% of white-coloured PVC polymer from the solid plastic waste. In this process, all additives (about



22% additives such as  $\text{CaCO}_3$  in PVC pipe) were removed from the PVC pipe waste.<sup>38</sup>

The extracted PVC was analysed and characterized by FT-IR spectroscopy, elemental analysis, and XPS. The results of the elemental analysis and XPS study showed the characteristic properties of the extracted PVC, which were identical to all the ideal properties of pure PVC. The percentage of carbon and hydrogen, as obtained from the elemental analysis of the extracted PVC, was very close to the theoretical percentage of carbon and hydrogen existing in pure PVC, respectively, which indicated the successful recovery and extraction of PVC polymer from solid plastic waste products such as PVC pipes. Treatment of the extracted PVC with ethylene diamine solution introduced the amine functionality into the structure of isolated PVC and resulted in the formation of aminated PVC (MPVC). The desired functionalized PVC material was characterized using different standard techniques such as FTIR, elemental analysis, and XPS study. The results of these standard analyses confirmed the amination of the extracted PVC. The appearance of a new FT-IR resonance band corresponding to the N–H stretching vibration apparently evidenced the inclusion of amine functionality within the structure of extracted PVC. The presence of nitrogen and its increase in abundance, as obtained from the elemental analysis, further confirmed the incorporation of the amine functionality in the structure of the PVC polymer. The formation of a characteristic new N 1s peak in the XPS spectra also confirmed the successful inclusion of the amine structural moiety in the extracted PVC material.

### 3.2 Characterization of extracted and modified PVC

A Shimadzu Fourier transform infrared spectrophotometer (FTIR-8400, wavenumber range of  $4000\text{ cm}^{-1}$  to  $400\text{ cm}^{-1}$ ) instrument was used to analyse the experimental samples. The FT-IR data showed different characteristic resonances at  $622.81\text{ cm}^{-1}$  for the C–Cl group,  $1429.97\text{ cm}^{-1}$  for the C–H group, and  $2919.08\text{ cm}^{-1}$  for the alkyl C–H functionality, which were identical to the corresponding bands observed in the pure PVC, confirming the successful extraction and isolation of PVC from the solid plastic waste (PVC waste pipes) (Fig. 2). The results of the FT-IR analysis of the extracted PVC were very similar to the data reported previously from the FT-IR resonances bands observed in the pure PVC polymer material.<sup>55</sup> Chemical treatment of the extracted PVC with ethylenediamine

solution yielded a functionalized material, which showed a new resonance band at  $3435.29\text{ cm}^{-1}$  in the FT-IR study.

The interesting and characteristic resonance at  $3435.29\text{ cm}^{-1}$  originated from the N–H stretching vibration, which apparently demonstrated the introduction of the amino functionality in the structure of the extracted PVC with the successful formation of the amino-PVC (APVC) material. It was observed that amination of the extracted PVC caused a decrease in the intensities of some resonance bands observed in the spectrum of pure PVC, whereas an increase in the intensity of the peak at  $1638.67\text{ cm}^{-1}$  was realized, corresponding to the C=C stretching vibration. This indicated that there might be some elimination reaction occurring simultaneously with the main substitution reaction, which effectively replaced the Cl group with the primary amine functionality in the resulting amino-PVC material.<sup>39</sup> The presence of  $\text{CO}_2$  might cause the appearance of an absorption peak at  $2347.00\text{ cm}^{-1}$  in the spectrum of the extracted PVC and at  $2349.46\text{ cm}^{-1}$  in the aminated PVC.<sup>56</sup> The chlorine content decreased as a result of the substitution reaction between PVC and the nucleophilic amine component of ethylenediamine (EDA) molecules, which led to a decrease in the intensity of the chlorine band in the respective spectra. In the XPS study, the powdered samples were mixed with ethanol, and the resulting mixtures were placed onto  $1 \times 1\text{ cm}^2$  glass slides and then subjected to spectroscopic analysis. A Thermo-Fisher Scientific XPS spectrometer ( $7 \times 10^{-7}$  mbar pressure) equipped with an Al  $k_\alpha$  anode ( $1486.68\text{ eV}$ ) as the X-ray source was used to record the XPS spectra of the experimental samples. A hemispherical capacitor analyser was utilized to collect the high-resolution scans of the elemental lines at a  $200\text{ eV}$  pass energy for the survey scans and  $50\text{ eV}$  pass energy for the narrow scans. These scans produced an Ag  $3d_{5/2}$  line full-width-at-half-maximum (FWHM) of less than  $1\text{ eV}$  and intensity above a linear background at BE from  $365\text{ eV}$  to  $371\text{ eV}$  using a  $1\text{ eV}$  average background. To illustrate the ultimate energy resolution of  $0.5\text{ eV}$ , other spectra were collected at a low pass energy ( $3\text{ eV}$ ). The Cu  $2p_{3/2}$ , Ag  $3d_{5/2}$ , and Au  $4f_{7/2}$  spectra showed the typical peak locations, which were used to calibrate the energy scale of the spectrometer. The peak positions were often observed within  $50\text{ meV}$  of the standard peak energies. The C 1s line of an adventitious hydrocarbon, with a binding energy (BE) of  $284.8\text{ eV}$ , served as the charge reference for the binding energies of the elemental lines. The Si 2p, Ca 2p, O 1s, and C 1s areas all had high-resolution spectra (narrow scans), as recorded for the experimental samples. The Avantage program was used to analyse the data and this software also provided the curve fitting and deconvoluted data. Fig. 3 displays the XPS spectra of PVC and APVC. The low-resolution (survey) XPS spectrum of PVC showed four peaks, which were C 1s around  $285\text{ eV}$ , O 1s around  $532\text{ eV}$ , Cl 2s around  $270\text{ eV}$  and Cl 2p around  $200\text{ eV}$ , whereas the corresponding spectrum of APVC consisted of five characteristics peaks, which were C 1s around  $285\text{ eV}$ , O 1s around  $532\text{ eV}$ , Cl 2s around  $270\text{ eV}$ , Cl 2p around  $200\text{ eV}$ , and N 1s around  $400\text{ eV}$ . The XPS spectra of both PVC and APVC showed traces of oxygen contamination in the respective materials. The results of the XPS analyses of the extracted PVC and APVC were highly comparable to the data reported from a study conducted previously on similar materials.<sup>57</sup>

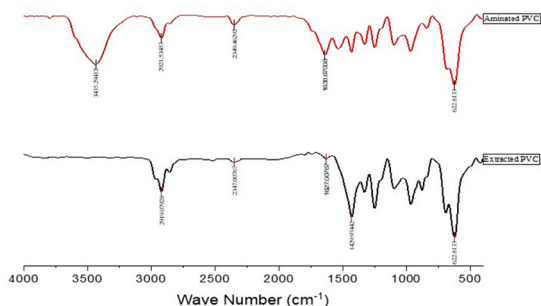


Fig. 2 FTIR spectra of the extracted and aminated PVC.



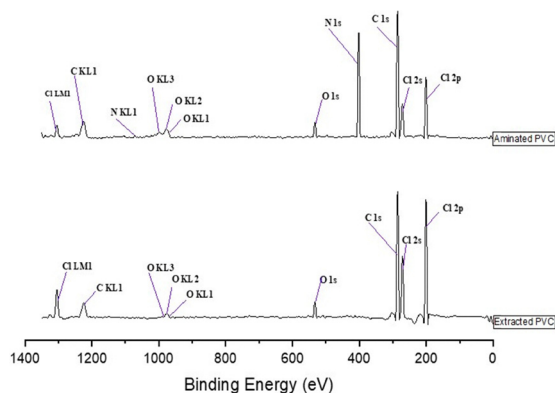


Fig. 3 XPS spectra of the extracted PVC and aminated PVC (APVC).

The XPS resonances at various binding energies observed in the spectra of the extracted PVC and APVC materials for the aforementioned elements were identical to the corresponding data obtained from similar materials synthesized previously by other research groups.<sup>56–60</sup> The appearance of an N 1s peak at around 400 eV in the XPS spectrum evidenced the incorporation of the amino functionality in the structure of the extracted PVC with the successful amination reaction, which effectively yielded APVC. The Cl/C and N/C ratios found in the PVC and APVC materials are listed in Table 1. The results showed that the amination treatment decreased the Cl/C ratio, whereas the N/C ratio increased in the resulting material, which demonstrated displacement of the chloro group by the amine functionality present in the ethylene diamine compound. The atomic percentage of chlorine was determined to be 23.59% in the extracted PVC and 11.16% in the aminated PVC. This finding demonstrates that around 47% of the chlorine atoms are replaced by nitrogen atoms throughout the amination process. The elemental analysis was carried out on the extracted PVC and APVC materials using a Vario Micro Cube (Germany) elemental analyser. The results of the elemental analysis showed that the percentage of nitrogen in APVC is 1.92%, whereas nitrogen was totally absent (zero) in the extracted PVC material, which further confirmed the successful amination of PVC to yield APVC. The results of all three standard analytical techniques (FT-IR, elemental, and XPS) confirmed the successful extraction of PVC from solid plastic waste as well as the effective modification of the structure of PVC with the incorporation of amine functionality by amination reaction, which displaced the chlorine group with the amine functionality present in ethylene diamine and yielded the amino-PVC polymer material (APVC). The reaction scheme for the modification and amination of the extracted PVC to synthesize the amino functional PVC material (APVC) is shown in Fig. 4.

Table 1 Elemental ratios in PVC and APVC based on the XPS data

Ratio	Cl/C	N/C
PVC	0.324663	0.000000
APVC	0.172088	0.311525

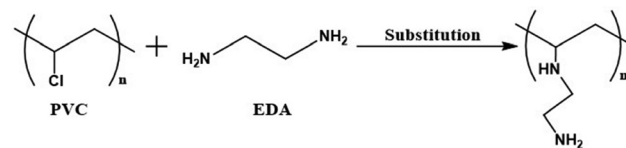


Fig. 4 Reaction scheme for the modification and amination of the extracted PVC.

### 3.3 Batch adsorption experiments

The modified amino-functionalized PVC (APVC) material was successfully applied as a potential adsorbent to remove and isolate methylene blue dye from different aqueous solutions utilizing adsorption technology. A series of batch experiments was conducted, where the appropriate amounts of APVC and methylene blue solution were mixed, and the resulting mixture was agitated using an orbital shaker at 180 rpm. The adsorbent dose, contact time, pH of the adsorbate solution, adsorption capacity of APVC, and efficiency of methylene blue on the surface of the adsorbent material were optimized accordingly. The detailed procedures for the optimization of all the experimental parameters for the effective removal of methylene blue from various aqueous solutions were described previously in the Experimental section. After the adsorption experiment, each mixture of adsorbent and MB solution was filtered to separate the solid APVC. The resultant filtrate was analysed for MB accordingly. The concentration of methylene blue in each aqueous solution before and after the adsorption experiment was determined using UV-Vis spectrophotometry.

**3.3.1 Effect of solution pH on the adsorption of MB on the surface of PVC and APVC.** The degree of ionization of the dye and sorbent surfaces depends on the extent of  $H^+$  ions present in the dye solution. Therefore, the surface characteristics and adsorption capabilities of adsorbents are significantly influenced by the pH of the analyte solution.<sup>61</sup> In this study, the initial methylene blue dye solution with a concentration of  $20 \text{ mg L}^{-1}$  at different pH was added separately to 10 mg of adsorbent per 20 mL adsorbate solution and the resulting mixture was agitated at  $30^\circ \text{C}$  for 15 h to examine the impact of pH on the adsorption of MB on PVC and APVC. The adsorption of methylene blue on the surface of APVC was found to be significantly influenced by a variation in the pH of the dye solution, as shown in Fig. 5. Methylene blue (MB) is a cationic dye that exists as positively charged ions in aqueous solution. The electrostatic repulsion between the positively charged surface of APVC (as amine groups protonated under acidic condition) and the positively charged MB molecules often makes it difficult for MB to get adsorbed on the surface of APVC adsorbent in acidic media (pH lower than 7), as observed in Fig. 5.

Similar effects of the pH of the analyte solution on the adsorption capacity of solid adsorbents were reported previously by Hermann *et al.*<sup>62</sup> The adsorption of MB on the surface of APVC was found to increase with an increase in the pH of the MB solution. The maximum removal of MB from the respective aqueous solutions by APVC was observed at



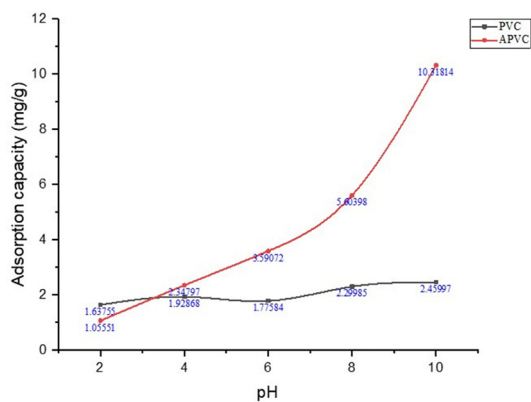


Fig. 5 Effect of solution pH on the adsorption of MB on the surface of APVC and extracted PVC.

pH 10, as demonstrated in Fig. 5. In the case of dye solution at pH = 10, almost all the amine groups within APVC existed in the deprotonated state, and thus free amine functionalities offer a convenient electron-rich environment for the binding of cationic MB dye species on the surface of APVC. At this stage, there were no available  $H^+$  ions in the MB solution that could compete with the cation groups of MB dye to be adsorbed on the surface of APVC, which resulted in the maximum adsorption of dye at pH 10.<sup>13</sup> The extracted PVC also showed MB adsorption on its surface to some extent, which increased with an increase in the pH of the respective solutions due to the dipolar attraction between the electronegative chloride group and cationic structural moiety of the MB dye species (Fig. 5). However, the extent of removal of MB from aqueous solution and the adsorption capacity of dye by PVC were significantly lower than that found with APVC, which demonstrated the efficiency of the amine functionality in the modified PVC (APVC) to extract and isolate MB dye from the aqueous solution. The occurrence of a minor degree of elimination reaction during the amination process of the extracted PVC might incorporate alkene groups to some extent within the structure of APVC in addition to the amine functionality, which might also enhance the adsorption of MB dye on the surface of APVC due to their  $\pi$ -interaction with the cationic charge density of MB molecules. Thus, the dye removal efficiency of APVC increased substantially in comparison to that found with the extracted pure PVC (Fig. 5). The results of MB removal from aqueous solutions by APVC were highly comparable to the data reported previously for the adsorption of MB on the surface of wood shavings.<sup>63</sup> Fig. 6 shows the stability profile of methylene blue dye in aqueous solutions at different pH.

Methylene blue was observed to be stable in aqueous solutions with a variation in pH from 2 to 10 and no structural degradation was realized within this pH range. However, the elevation of solution pH above 10 caused the degradation of MB in the respective solution, as demonstrated in Fig. 6. Therefore, all the adsorption experiments for the effective removal of MB from aqueous solution were carried out in the pH range of 2 to 10 (Fig. 6).

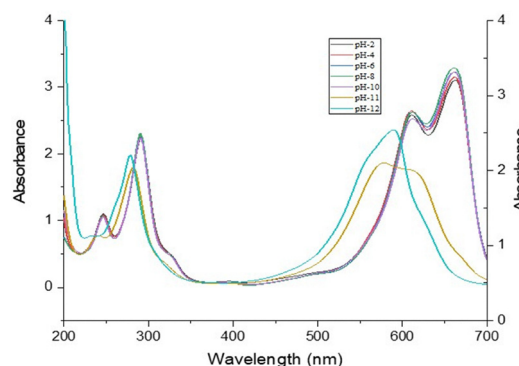


Fig. 6 pH profile of methylene blue (MB) solutions.

**3.3.2 Effect of initial adsorbate concentration on the removal of MB by PVC and APVC.** The degree of MB removal from aqueous solutions by APVC and PVC was examined in terms of adsorption capacity ( $q_e$ ) and % removal. However, these significant parameters in the dye adsorption process were greatly influenced by the initial dye concentration, as illustrated in Fig. 7. The percentage of dye removal and separation from aqueous solutions showed an inverse relationship to the respective dye concentration, where the percentage of dye removal decreased with an increase in the initial dye concentration.

Though the percent MB adsorption on PVC and APVC decreased with an increase in the initial dye concentration, the actual amount of dye adsorbed per unit mass of adsorbent (adsorption capacity,  $q_e$ ) increased with an increase in the dye concentration in the experimental solutions and adsorption equilibrium was assumed to be established eventually in the respective MB-adsorbent mixtures. The concentration gradient that was created between the dye solution and the surface of the adsorbent worked as a driving force for the equilibrium process, which might result in an increase in the adsorption capacity ( $q_e$ ) of APVC with an increase in the dye concentration in aqueous solutions. When all the active sites on the surfaces of APVC and PVC were occupied by MB species, adsorption equilibrium was established between the adsorbent and adsorbed species.<sup>61,64</sup> Thus, the surface of the adsorbent became saturated and no potential active sites were available

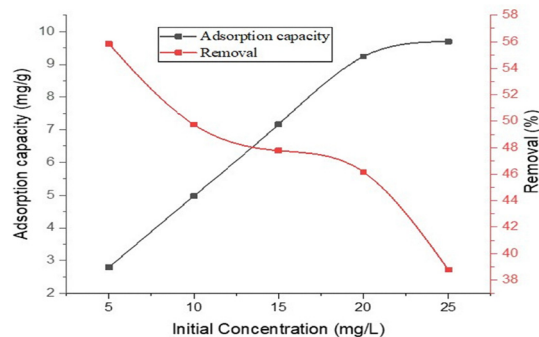


Fig. 7 Influence of the initial concentration of dye on the adsorption of MB onto APVC.



to bind MB species from higher concentrated dye solutions. Similar findings for the removal of dyes by solid adsorbents were documented previously in the literature.<sup>65,66</sup>

**3.3.3 Effect of contact time on the adsorption of MB on PVC and APVC.** The adsorption experiments were carried out for different periods of times to investigate the effect of contact time on the adsorption of MB on the surface of APVC and PVC and the results are illustrated in Fig. 8. A rapid rise in the extent of dye effectively removed by APVC from aqueous solution was realized when the contact time was increased from 1 h to 7 h during the experimental adsorption processes. The adsorption capacity ( $q_e$ ) of APVC was found to increase from 2.46 to 9.37 mg g<sup>-1</sup> during this time, while the MB removal percentage was also observed to be elevated from 12.28% to 46.83%. In the initial stage of the adsorption experiment, the surface of APVC exposed a higher number of accessible active sites, which potentially could bind MB molecules in to a greater extent with an increase in the contact time.

However, the surface of APVC eventually became saturated with MB species with an increase in the contact time between MB species and APVC adsorbent, and at 11 h the adsorption process reached the equilibrium state. At this point, the highest amount of MB species was bound on the adsorbent surface, which was demonstrated with the maximum MB removal percentage of 46.83%, where the adsorption process was stabilized and an equilibrium stage between MB species and APVC appeared in the respective mixtures. After the equilibrium saturation phase and above the experimental contact time of 11 h, the adsorption capacity of APVC and the MB removal percentage decreased as most of the active sites were occupied by MB species, and apparently there were no available sites on the surface of the adsorbent to bind the respective dye species.<sup>67</sup> The results of interaction time of MB with APVC in the adsorption processes as well as the corresponding MB removal efficiency of the adsorbent with the percentage removal of MB from the respective solutions showed an identical trend to the data reported in similar studies conducted previously by other research groups.<sup>68</sup>

**3.3.4 Effect of adsorbent dose on the removal of MB by PVC and APVC from aqueous solutions.** In this study, different

quantities of adsorbents (APVC) were applied, while keeping the concentration of the MB solution constant throughout the adsorption process to investigate the efficiency of MB removal from different aqueous solutions and the results are displayed in Fig. 9. The adsorption capacity ( $q_e$ ) of APVC was observed to decrease from 12.48 to 3.69 mg g<sup>-1</sup> with an increase in the amount of adsorbent in the respective experimental adsorption processes. There might be accumulation or overlapping of the adsorption sites, which could reduce the extent of overall adsorbent surface area accessible to methylene blue species, and thus interrupted the MB adsorption equilibrium processes in the respective system.<sup>69</sup>

However, the percentage removal of MB from aqueous solution gradually increased with an increase in the adsorbent dosage during the adsorption experiments, and then it reached the maximum point, and thereafter dropped with a further increase in the adsorbent dose. There might be more exposed available surface area with a higher abundance of active sites with an increase in the quantity of APVC adsorbent, which might result in an elevation of the percent removal of MB from the respective solutions.<sup>13</sup> The maximum percent removal of MB was found with 10 mg of adsorbent APVC applied in 10 mL of MB solution, whereas the highest adsorption capacity was measured at 5 mg of adsorbent per 10 mL of MB solution. Evaluation of the adsorption capacity and percent removal of MB from aqueous solutions showed that the optimized adsorbent dose (APVC) is 10 mg applied into 10 mL of MB solution at the optimized initial analyte concentration, contact time, and pH.

#### 3.4 Possible mechanistic scheme for MB removal by APVC

APVC has amine groups, while methylene blue contains nitrogen with a lone pair of electrons. Thereby, the structures of both APVC and MB provide active sites for hydrogen bond formation. In this way, MB adsorption on APVC occurs *via* hydrogen bonding. The amine groups in modified PVC at pH 10 remain deprotonated, and hence the nitrogen atom functions as a negative centre, while methylene blue is a cationic dye even at this high pH. Given that electrostatic interaction is found between all oppositely charged centres, the electrostatic

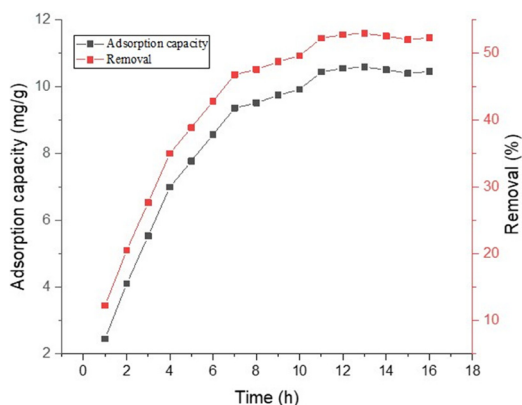


Fig. 8 Influence of contact time on the adsorption of MB onto APVC.

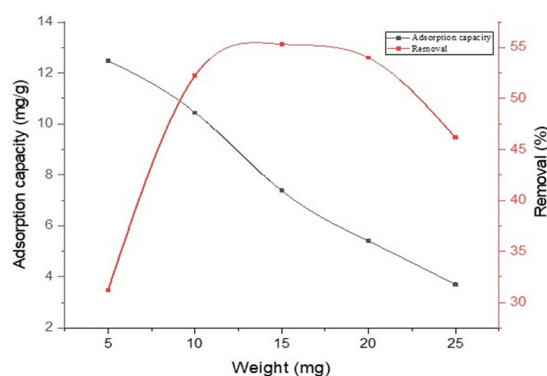


Fig. 9 Influence of adsorbent dose on the adsorption of MB onto the surface of APVC.



interaction between APVC and MB is also a driving force for the adsorption of MB on modified PVC. Additionally, the removal efficiency further increased by the van der Waals interaction between the dye and adsorbent. A possible mechanistic scheme for methylene blue adsorption on aminated PVC is shown in Scheme 1.

### 3.5 Statistical analysis of MB adsorption on the surface of APVC

**3.5.1 Isotherm modelling study.** Three different isotherm models, *i.e.*, Langmuir, Freundlich, and Temkin isotherm models, were utilized to examine the relationship between equilibrium dye uptake ( $q_e$ ) and final concentration of MB in the equilibrium state ( $C_e$ ), which might directly impact the adsorption of MB on the surface of APVC. The data obtained from MB removal by APVC from aqueous solution following the characteristic adsorption experiments were plugged in to these three isotherm model equations. The magnitudes of the different parameters related to the three isotherm models were calculated accordingly, and the results are displayed in Table 2. The data in Table 2 indicates that the magnitude of  $R^2$  obtained from the Langmuir model is 0.9699 which, is significantly higher than that observed from the application of the Freundlich model (0.8882) and Temkin model (0.8043), respectively. The results of MB removal from aqueous solution by APVC were best fitted to the Langmuir model, and among the three models, it was found to be most suitable to describe the isothermal characteristics of MB adsorption on the surface of APVC.

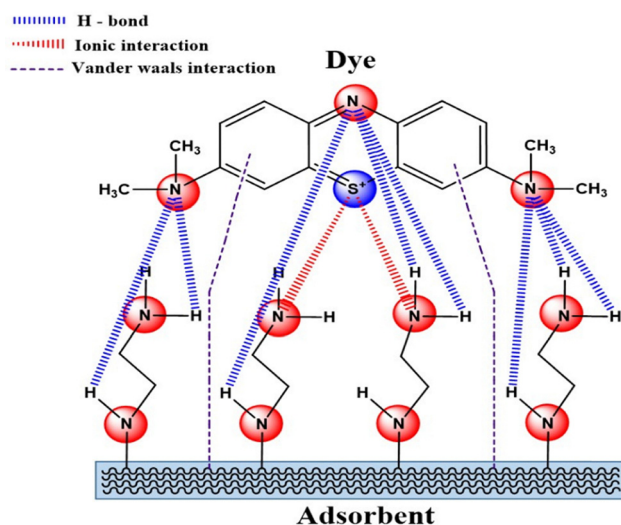
**3.5.1.1 Langmuir isotherm study.** The magnitude of the Langmuir constant ( $R_L$ ) explains the nature and deviation of an adsorption process, where it is unfavourable ( $R_L > 1$ ), linear ( $R_L = 1$ ), favourable ( $0 < R_L < 1$ ), or irreversible ( $R_L = 0$ ).<sup>42</sup> In the present study, the value of  $R_L$  at equilibrium was recorded to be 0.4931, which apparently indicated that MB adsorption on the surface of APVC was a highly favourable process (Table 2). The

Table 2 Magnitude of various parameters from different adsorption isotherm models obtained for MB adsorption on the surface of APVC

Isotherm	Parameter	Value
Langmuir isotherm	$q_{\max}$ ( $\text{mg g}^{-1}$ )	21.04
	$K_L$	0.0685
	$R_L$	0.4931
	$R^2$	0.9699
Freundlich isotherm	$1/n$	0.7133
	$K_f$	1.6473
	$R^2$	0.8882
Temkin isotherm	$B_T$ ( $\text{J mol}^{-1}$ )	4.0821
	$A_T$ ( $\text{L mg}^{-1}$ )	0.8487
	$R^2$	0.8043

magnitudes of  $q_{\max}$  and  $K_L$  for MB adsorption on APVC were 21.04  $\text{mg g}^{-1}$  and 0.0685, respectively, as obtained from the utilization of the Langmuir isotherm equation. The extent of all the Langmuir parameters obtained from the experimental system suggested the effective removal of MB by APVC from aqueous solutions following adsorption technology.

**3.5.1.2 Freundlich isotherm and Temkin isotherm study.** The Freundlich isotherm model was utilized to explain the nature of adsorption occurring in the removal of MB from aqueous solutions by APVC. The value of  $R^2$  obtained by plugging the experimental data from MB adsorption on the APVC surface was 0.8882. The magnitude of  $n$  associated with the Freundlich isotherm equation was calculated by utilizing the value of  $R^2$ . It could be anticipated that the adsorption of MB on the surface of APVC might occur through a chemisorption or physisorption process. The value of  $n$  can effectively predict the affinity of the adsorption process as either chemisorption ( $n < 1$ ) or physisorption ( $n > 1$ ).<sup>46</sup> In the present investigation, the value of  $1/n$  was calculated to be 0.7133, indicating the occurrence of physisorption, which resulted in the removal of MB species from aqueous solution by APVC. In general, physisorption processes are driven by van der Waals forces, which occur between the adsorbate molecules and the surface functionalities of adsorbent materials. A magnitude of  $n$  lower than 0.5 suggests a low adsorption intensity, while the corresponding



Scheme 1 Schematic of MB adsorption on APVC.

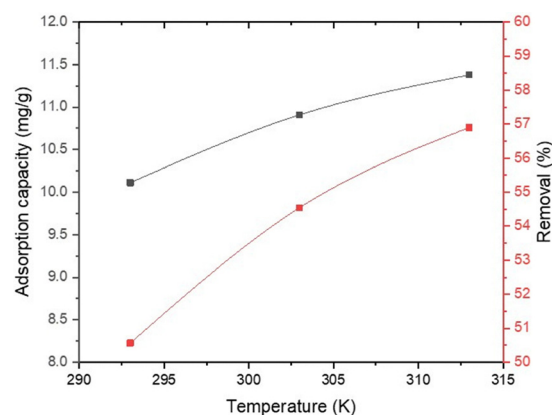


Fig. 10 Influence of temperature on the adsorption of MB onto APVC.



values between 2 and 10 indicate the occurrence of strong adsorption.<sup>46</sup> The value of  $n$  obtained in the present study was 1.4019, which apparently indicated the effective adsorption of MB on the surface of APVC, resulting in the successful extraction and separation of MB species from different aqueous solutions by APVC. The experimental MB adsorption data were also plugged into the Temkin isotherm model equation and the magnitude  $R^2$  was calculated to be 0.8043, which suggested the existence of good interactions between the MB species and surface functionalities of APVC.<sup>70</sup> The results of MB adsorption on APVC did not demonstrate a very good fit with the Temkin isotherm model in comparison to the Freundlich isotherm model, as indicated by the  $R^2$  value (0.8043). The magnitude of  $A_T$  displayed in Table 2 showed the greater affinity of the adsorbent for the MB dye molecules, which caused the separation of MB species from aqueous solution.

### 3.5.2 Thermodynamic study of MB adsorption on APVC.

All adsorption experiments were carried out at different temperatures such as 20 °C, 30 °C, and 40 °C (293, 303 and 313 K, respectively) to investigate the variation in MB removal from aqueous solutions by APVC with a change in temperature. The adsorption capability of MB onto APVC was found to increase slowly with an increase in the experimental temperature from 20 °C to 40 °C (Fig. 10). Elevation of experimental temperature might cause an increase in the activation energy of adsorbate species and mass transfer kinetics in the adsorption system, which might enhance the adsorption capacity of APVC as well as MB percentage removal, as shown in Fig. 10.<sup>42</sup> However, an increase in the experimental temperature from 30 °C to 40 °C did not significantly elevate the adsorption capacity (about 5%) of APVC and MB removal percentage (about 4%) from aqueous solutions (Fig. 10). Thus, considering energy consumption, 30 °C (room temperature) was considered as the optimized temperature for the MB adsorption experiments. Different significant thermodynamic parameters such as  $\Delta G^\circ$ ,  $\Delta H^\circ$ , and  $\Delta S^\circ$  were determined for the adsorption of MB on the surface of APVC and the results are summarized in Table 3. All the values of  $\Delta G^\circ$  measured at three distinct experimental temperatures (293, 303, and 313 K) were found to be negative (Table 3), indicating the spontaneous nature of MB adsorption on the surface of APVC. The magnitude of  $\Delta G^\circ$  appeared as negative and it was observed to decrease from  $-0.0551$  to  $-0.7229$  kJ mol<sup>-1</sup> as the experimental temperature increased, which suggested that the MB removal from aqueous solutions by APVC was relatively favourable at higher temperatures. The trend in the change in  $\Delta G^\circ$  found for MB adsorption on the surface of APVC during the present study was highly comparable to the data reported previously in a similar study.<sup>49</sup> The

**Table 3** Magnitude of different thermodynamic parameters determined for the adsorption of MB on APVC

Temperature (K)	$\Delta G^\circ$ (kJ mol <sup>-1</sup> )	$\Delta H^\circ$ (kJ mol <sup>-1</sup> )	$\Delta S^\circ$ (J K <sup>-1</sup> mol <sup>-1</sup> )
293	-0.0551	9.7524	33.5474
303	-0.4594		
313	-0.7229		

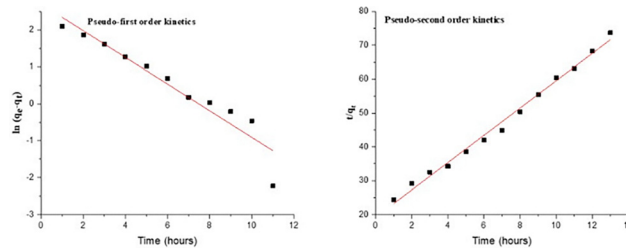


**Fig. 11** Evaluation of MB adsorption kinetics with the application of pseudo-first order and pseudo-second-order kinetic models.

slope and intercept of the van't Hoff plot of  $\ln(K_L)$  vs.  $1/T$  were used to calculate  $\Delta H^\circ$  and  $\Delta S^\circ$ .<sup>45,71,72</sup> The enthalpy change appeared to be positive, revealing the endothermic nature of the MB adsorption process on APVC.<sup>43,48</sup>

The magnitude of entropy change ( $\Delta S^\circ > 0$ ) was found to be positive, which suggested an increase in the randomness and disorder of solid-liquid phase adsorption as well as energy redistribution in the respective process associated with the removal of MB from different aqueous solutions by APVC.<sup>43</sup>

### 3.5.3 Kinetic study of MB removal from aqueous solutions by APVC.

Both pseudo-first order (PFO) and pseudo-second-order (PSO) kinetic models were utilized to evaluate the adsorption kinetics associated with MB removal by APVC. All experimental data were plugged into the PFO and PSO model equations and the results were analysed accordingly. The data were found to be fitted linearly, which demonstrated that MB adsorption on the surface of APVC followed pseudo-second-order (PSO) kinetics, rather than the pseudo-first-order (PFO) phenomenon (Fig. 11). The magnitude of  $R^2$  determined from the straight line equation obtained from the application of the MB adsorption data in the pseudo-second-order model was found to be closer to 1 in comparison to that observed from the analysis of the pseudo-first-order kinetic model. The results of the PSO kinetic model study suggested that the MB adsorption rate was dependent on both  $q_t$  (adsorption capacity at any time  $t$ ) and  $q_e$  (adsorption capacity at equilibrium time).<sup>73</sup>

The kinetic analysis data indicated that the findings of MB removal from aqueous solutions were best fitted to the pseudo-second-order kinetic model with the formation of a linear straight line, which showed good agreement with the magnitude of the correlation coefficient  $R^2$  of 0.9914. The theoretical MB adsorption capacity of APVC obtained from the application of PFO was 14.8359 mg g<sup>-1</sup> and from PSO was 14.8876 mg g<sup>-1</sup>, which were very close to the corresponding adsorption capacity

**Table 4** Magnitudes of various kinetic parameters determined for the adsorption of MB on the surface of APVC

Kinetics	Parameter	Unit	Value
Pseudo-first-order kinetics	$q_e$	(mg g <sup>-1</sup> )	14.8359
	$K_1$	(h <sup>-1</sup> )	0.0328
	$R^2$	—	0.9013
Pseudo-second-order kinetics	$q_e$	(mg g <sup>-1</sup> )	14.8876
	$K_2$	(g mg <sup>-1</sup> h <sup>-1</sup> )	0.8439
	$R^2$	—	0.9914



of APVC found experimentally ( $12.4838 \text{ mg g}^{-1}$ ). Notably, the magnitudes of both kinetic constants  $K_1$  and  $K_2$  were very low (Table 4), suggesting the slow rate of MB adsorption equilibrium on the surface of APVC, which was consistent with the experimental reaction time of 12 h realized to establish adsorption equilibrium between the MB species and functional moieties on the PVC surface during the MB removal process.

## 4. Conclusions

Herein, an amino-functionalized polymer material was synthesized from waste PVC pipes and characterized from the perspectives of solid plastic waste management and clean environment. This amino-functionalized PVC material was successfully applied as a potential adsorbent in dye removal technology. PVC was separated and isolated from waste PVC pipes in good yield *via* the solvent extraction method using THF solvent. Amine functionality was introduced into the extracted PVC structure by treating it with ethylenediamine (EDA). The product (APVC) was characterized using different standard analytical techniques such as FT-IR spectroscopy, elemental analysis, and XPS. APVC was utilized to remove methylene blue (MB) dye from different aqueous solutions by conducting a series of adsorption experiments. APVC effectively removed and isolated MB dye from the aqueous solutions with the optimized solution pH, contact time, initial dye concentration, and temperature, where all these parameters showed significant impacts on the MB removal process. The application of the Langmuir isotherm model provided the logical description of the MB adsorption equilibrium on the surface of APVC with monolayer formation. The MB adsorption data were observed to be best suited to the pseudo-second-order model, indicating the kinetics of MB removal from aqueous solutions.

The spontaneous nature of the MB adsorption process on the surface of APVC was demonstrated by the appearance of a negative Gibbs free energy ( $\Delta G^\circ$ ), whereas the positive magnitudes of both the entropy ( $\Delta S^\circ$ ) and enthalpy changes suggest the randomness and exothermic characteristics of the MB removal process from aqueous solutions, respectively. The significant findings of this study will be highly useful for minimizing solid plastic waste and toxic dye pollution in the terrestrial environment as well as in developing and building cost-effective wastewater treatment techniques for the removal of toxic dyes from various industrial effluents.

## Author contributions

Lokman Hosen: investigation, formal analysis, data curation, software and writing original draft. Md Abdul Goni: conceptualization, methodology, project administration, supervision and writing – review and editing the manuscript. Most. Johura Khatun: investigation, formal analysis and data curation. Sharmeen Nishat: conceptualization, methodology, project administration, resources, supervision and writing – review and editing the manuscript.

## Conflicts of interest

There are no conflicts to declare.

## Data availability

All the data generated and analysed during this research have been included in this article.

## Acknowledgements

The authors would like to express their sincere gratitude to the Department of Chemistry at Bangladesh University of Engineering and Technology (BUET) for providing the necessary instrumental supports during this research. The authors also gratefully acknowledge the Postgraduate Fellowship of CASR and the Basic Research Grant, BUET, for funding this research.

## References

- 1 A. Ayub, Z. A. Raza, M. I. Majeed, M. R. Tariq and A. Irfan, Development of sustainable magnetic chitosan biosorbent beads for kinetic remediation of arsenic contaminated water, *Int. J. Biol. Macromol.*, 2020, **163**, 603–617.
- 2 S. Sarkar, S. S. Gill, G. Das Gupta and S. Kumar Verma, Water toxicants: a comprehension on their health concerns, detection, and remediation, *Environ. Sci. Pollut. Res.*, 2022, **29**(36), 53934–53953.
- 3 X. Y. Zou, X. Y. Peng, X. X. Zhao and C. P. Chang, The impact of extreme weather events on water quality: international evidence, *Nat. Hazards*, 2023, **115**(1), 1–21, DOI: [10.1007/s11069-022-05548-9](https://doi.org/10.1007/s11069-022-05548-9).
- 4 K. Sunil, P. Sherugar, S. Rao, C. Lavanya, G. R. Balakrishna, G. Arthanareeswaran and M. Padaki, Prolific approach for the removal of dyes by an effective interaction with polymer matrix using ultrafiltration membrane, *J. Environ. Chem. Eng.*, 2021, **9**(6), 106328, DOI: [10.1016/j.jece.2021.106328](https://doi.org/10.1016/j.jece.2021.106328).
- 5 N. Athira and D. S. Jaya, Effects of tartrazine on growth and brain biochemistry of Indian major carps on long-term exposure, *Int. J. Adv. Biochem. Res.*, 2022, **6**(2), 25–33.
- 6 A. Zand, S. Enkhbilguun, J. M. Macharia, F. Budán, Z. Gyöngyi and T. Varjas, Tartrazine modifies the activity of DNMT and HDAC genes—is this a link between cancer and neurological disorders?, *Nutrients*, 2023, **15**(13), 2946, DOI: [10.3390/nu15132946](https://doi.org/10.3390/nu15132946).
- 7 D. Shen, J. Fan, W. Zhou, B. Gao, Q. Yue and Q. Kang, Adsorption kinetics and isotherm of anionic dyes onto organo-bentonite from single and multisolute systems, *J. Hazard. Mater.*, 2009, **172**(1), 99–107.
- 8 H. A. Alalwan, M. A. Kadhom and A. H. Alminshid, Removal of heavy metals from wastewater using agricultural byproducts, *J. Water Supply: Res. Technol. – AQUA*, 2020, **69**(2), 99–112.
- 9 K. Kadirvelu, M. Kavipriya, C. Karthika, M. Radhika, N. Vennilamani and S. Pattabhi, Utilization of various agricultural wastes for activated carbon preparation and



- application for the removal of dyes and metal ions from aqueous solutions, *Bioresour. Technol.*, 2003, **87**(1), 129–132.
- 10 M. Kadhom, N. Albayati, H. Alalwan and M. Al-Furaiji, Removal of dyes by agricultural waste, *Sustain. Chem. Pharm.*, 2020, **16**, 100259, DOI: [10.1016/j.scp.2020.100259](https://doi.org/10.1016/j.scp.2020.100259).
  - 11 Y. Song, L. Wang, X. Qiang, W. Gu, Z. Ma and G. Wang, An overview of biological mechanisms and strategies for treating wastewater from printing and dyeing processes, *J. Water Process Eng.*, 2023, **55**, 104242, DOI: [10.1016/j.jwpe.2023.104242](https://doi.org/10.1016/j.jwpe.2023.104242).
  - 12 S. T. Yang, S. Chen, Y. Chang, A. Cao, Y. Liu and H. Wang, Removal of methylene blue from aqueous solution by graphene oxide, *J. Colloid Interface Sci.*, 2011, **359**(1), 24–29.
  - 13 N. Nasuha, B. H. Hameed and A. T. M. Din, Rejected tea as a potential low-cost adsorbent for the removal of methylene blue, *J. Hazard. Mater.*, 2010, **175**(1–3), 126–132.
  - 14 E. N. Mohamed, A. I. A. Elhamid, A. A. El Bardan, H. M. A. Soliman and M. S. M. Eldin, Development of carboxymethyl cellulose – graphene oxide biobased composite for the removal of methylene blue cationic dye model contaminate from wastewater, *Sci. Rep.*, 2023, **13**(1), 14265, DOI: [10.1038/s41598-023-41431-8](https://doi.org/10.1038/s41598-023-41431-8).
  - 15 A. Simi and V. Azeeza, Removal of methylene blue dye using low cost adsorbent, *Asian J. Chem.*, 2010, **22**(6), 4371–4376.
  - 16 W. J. Cosgrove and D. P. Loucks, Water management: Current and future challenges and research directions, *Water Resour. Res.*, 2015, **51**(6), 4823–4839.
  - 17 A. T. Hoang, S. Kumar, E. Lichtfouse, C. K. Cheng, R. S. Varma, N. Senthilkumar, P. Q. P. Nguyen and X. P. Nguyen, Remediation of heavy metal polluted waters using activated carbon from lignocellulosic biomass: an update of recent trends, *Chemosphere*, 2022, **302**, 134825, DOI: [10.1016/j.chemosphere.2022.134825](https://doi.org/10.1016/j.chemosphere.2022.134825).
  - 18 H. Zhang, S. Pap, M. A. Taggart, K. G. Boyd, N. A. James and S. W. Gibb, A review of the potential utilisation of plastic waste as adsorbent for removal of hazardous priority contaminants from aqueous environments, *Environ. Pollut.*, 2020, **258**, 113698, DOI: [10.1016/j.envpol.2019.113698](https://doi.org/10.1016/j.envpol.2019.113698).
  - 19 M. A. Keane, Catalytic conversion of waste plastics: focus on waste PVC, *J. Chem. Technol. Biotechnol.*, 2007, **82**, 787–795.
  - 20 A. A. Ameer, M. S. Abdallah, A. A. Ahmed and E. A. Yousif, Synthesis and characterization of polyvinyl chloride chemically modified by amines, *Open J. Polym. Chem.*, 2013, **3**(1), 11–15.
  - 21 S. S. Ghaisas, D. D. Kale, J. G. Kim and B. W. Jo, Blends of plasticized poly(vinyl chloride) and waste flexible poly(vinyl chloride) with waste nitrile rubber powder, *J. Appl. Polym. Sci.*, 2004, **91**(3), 1552–1558.
  - 22 W. Arayaprane, P. Prasassarakich and G. L. Rempel, Blends of Poly(Vinyl chloride) PVQ/natural rubber-g-(styrene-co-methyl methacrylate) for improved impact resistance of PVC, *J. Appl. Polym. Sci.*, 2004, **93**(4), 1666–1672.
  - 23 K. Bierbrauer, M. López-González, E. Riande and C. Mijangos, Gas transport in fluorothiophenyl modified PVC membranes, *J. Membr. Sci.*, 2010, **362**(1–2), 164–171.
  - 24 S. Bigot, G. Louarn, N. Kébir and F. Burel, Straightforward approach to graft bioactive polysaccharides onto polyurethane surfaces using an ionic liquid, *Appl. Surf. Sci.*, 2014, **314**, 301–307.
  - 25 D. Braun, Poly(vinyl chloride) on the way from the 19th century to the 21st century, *J. Polym. Sci., Part A: Polym. Chem.*, 2004, **42**(3), 578–586.
  - 26 M. Knot and K. Mulder, PVC plastic: a history of systems development and entrenchment, *Technol. Soc.*, 2001, **23**(2), 265–286.
  - 27 J. I. Mnyango and S. P. Hlangothi, Polyvinyl chloride applications along with methods for managing its end-of-life items: a review, *Prog. Rubber, Plast. Recycl. Technol.*, 2024, 14777606241308652, DOI: [10.1177/14777606241308652](https://doi.org/10.1177/14777606241308652).
  - 28 H. Stichnothe and A. Azapagic, Life cycle assessment of recycling PVC window frames, *Resour., Conserv. Recycl.*, 2013, **71**, 40–47, DOI: [10.1016/j.resconrec.2012.12.005](https://doi.org/10.1016/j.resconrec.2012.12.005).
  - 29 M. Sadat-Shojai and G. R. Bakhshandeh, Recycling of PVC wastes, *Polym. Degrad. Stab.*, 2011, **96**(4), 404–415.
  - 30 D. Garcia, R. Balart, J. E. Crespo and J. Lopez, Mechanical properties of recycled PVC blends with styrenic polymers, *J. Appl. Polym. Sci.*, 2006, **101**(4), 2464–2471.
  - 31 A. S. Ditta, A. J. Wilkinson, G. M. McNally and W. R. Murphy, A study of the processing characteristics and mechanical properties of multiple recycled rigid PVC, *J. Vinyl Addit. Technol.*, 2004, **10**(4), 174–178.
  - 32 T. Yoshioka, K. Furukawa and A. Okuwaki, Chemical recycling of rigid-PVC by oxygen oxidation in NaOH solutions at elevated temperatures, *Polym. Degrad. Stab.*, 2000, **67**(2), 285–290.
  - 33 C. H. Wu, C. Y. Chang, J. L. Hor, S. M. Shih, L. W. Chen and F. W. Chang, Two-Stage pyrolysis model of PVC, *Can. J. Chem. Eng.*, 1994, **72**(4), 644–650.
  - 34 A. Ouerghui, F. Ammari and C. Girard, The use of chemically modified PVC waste to remove ions from wastewater, *Polimery*, 2020, **65**(11–12), 801–806.
  - 35 N. A. Alrazzak, S. A. Aowda and A. J. Atiyah, Removal of bismarck brown G dye from aqueous solution over a composite of triazole-polyvinyl chloride polymer and zinc oxide, *Orient. J. Chem.*, 2017, **33**(5), 2476–2483.
  - 36 A. U. Ahmed, H. Ibraheem, M. Kadhom, A. A. Rashad, W. H. Al-dahhan and M. Bufaroosha, Modified PVC as adsorbent for methyl orange dye removable, *AIP Conf. Proc.*, 2022, **2450**(1), 020006, DOI: [10.1063/5.0093582](https://doi.org/10.1063/5.0093582).
  - 37 F. Mbarki, H. Al Batin, F. Mbarki and H. Al Batin, Chemical modification of commercial and recovered poly(vinyl chloride) with amino groups – adsorption of heavy metals (Cr(III), Pb(II), Cd(II), OR Co(II)) by modified pvc polymers, *J. Mar. Chim. Heterocycl.*, 2021, **20**(2), 80–94.
  - 38 W. M. Qiao, Y. Song, S. H. Yoon, Y. Korai, I. Mochida and O. Katou, Preparation of PVC pitch from waste pipe, *Carbon*, 2005, **43**(9), 2022–2025.
  - 39 E. J. Park, B. C. Park, Y. J. Kim, A. Canlier and T. S. Hwang, Elimination and substitution compete during amination of poly(vinyl chloride) with ethylenediamine: XPS analysis and approach of active site index, *Macromol. Res.*, 2018, **26**(10), 913–923.
  - 40 M. Landarani, M. Arab Chamjangali and B. Bahramian, Preparation and characterization of a novel chemically



- modified PVC adsorbent for methyl orange removal: optimization, and study of isotherm, kinetics, and thermodynamics of adsorption process, *Water, Air, Soil Pollut.*, 2020, **231**(10), 513, DOI: [10.1007/s11270-020-04874-7](https://doi.org/10.1007/s11270-020-04874-7).
- 41 G. Zhu, C. Zhang, K. Li, X. Xi, X. Zhang and H. Lei, A multifunctional zeolitic imidazolate framework-8@wood aerogel composite intergrating superior performance of dye adsorption capacity and flame-retardant property, *J. Porous Mater.*, 2023, **30**(4), 1171–1182.
- 42 H. Jain, V. Yadav, V. D. Rajput, T. Minkina, S. Agarwal and M. C. Garg, An eco-sustainable green approach for biosorption of methylene blue dye from textile industry wastewater by sugarcane bagasse, peanut hull, and orange peel: a comparative study through response surface methodology, isotherms, kinetic, and thermodynamics, *Water, Air, Soil Pollut.*, 2022, **233**(6), 187, DOI: [10.1007/s11270-022-05655-0](https://doi.org/10.1007/s11270-022-05655-0).
- 43 X. Guo, W. Hu, Z. Gu, J. Li, Z. Xie, C. Fang and H. Tao, Enhanced removal of aqueous chromium(vi) by KOH-activated soybean straw-based carbon, *Water, Air, Soil Pollut.*, 2021, **232**(12), 484, DOI: [10.1007/s11270-021-05435-2](https://doi.org/10.1007/s11270-021-05435-2).
- 44 J. Kim, G. H. Bak, D. Y. Yoo, Y. I. Lee, Y. G. Lee and K. Chon, Functionalization of pine sawdust biochars with Mg/Al layered double hydroxides to enhance adsorption capacity of synthetic azo dyes: Adsorption mechanisms and reusability, *Heliyon*, 2023, **9**(3), DOI: [10.1016/j.heliyon.2023.e14142](https://doi.org/10.1016/j.heliyon.2023.e14142).
- 45 A. Murugesan, M. Divakaran, P. Raveendran, A. B. Nitin Nikamant and K. J. Thelley, An eco-friendly porous poly(imide-ether)s for the efficient removal of methylene blue: adsorption kinetics, isotherm, thermodynamics and reuse performances, *J. Polym. Environ.*, 2019, **27**(5), 1007–1024.
- 46 K. A. M. Said, N. Z. Ismail, R. L. Jama'in, N. A. M. Alipah, N. M. Sutan, G. G. Gadung, R. Baini and N. S. A. Zauzi, Application of freundlich and Temkin isotherm to study the removal of Pb(II) via adsorption on activated carbon equipped polysulfone membrane, *Int. J. Eng. Technol.*, 2018, **7**(3.18), 91–93.
- 47 A. A. Khan and R. P. Singh, Adsorption thermodynamics of carbofuran on Sn(IV) arsenosilicate in H<sup>+</sup>, Na<sup>+</sup> and Ca<sup>2+</sup> forms, *Colloids Surf.*, 1987, **24**(1), 33–42.
- 48 A. Ramesh, D. J. Lee and J. W. C. Wong, Thermodynamic parameters for adsorption equilibrium of heavy metals and dyes from wastewater with low-cost adsorbents, *J. Colloid Interface Sci.*, 2005, **291**(2), 588–592.
- 49 Y. Dong, M. Gao, Z. Song and W. Qiu, As(III) adsorption onto different-sized polystyrene microplastic particles and its mechanism, *Chemosphere*, 2020, **239**, 124792, DOI: [10.1016/j.chemosphere.2019.124792](https://doi.org/10.1016/j.chemosphere.2019.124792).
- 50 A. Aurich, J. Hofmann, R. Oltrogge, M. Wecks, R. Gläser, L. Blömer, S. Mauersberger, R. A. Müller, D. Sicker and A. Giannis, Improved isolation of microbiologically produced (2r,3s)-isocitric acid by adsorption on activated carbon and recovery with methanol, *Org. Process Res. Dev.*, 2017, **21**(6), 866–870.
- 51 Z. Fang, Y. Gao, F. Zhang, K. Zhu, Z. Shen, H. Liang, Y. Xie, C. Yu, Y. Bao, B. Feng, N. Bolan and H. Wang, The adsorption mechanisms of oriental plane tree biochar toward bisphenol S: a combined thermodynamic evidence, spectroscopic analysis and theoretical calculations, *Environ. Pollut.*, 2022, **310**, 119819, DOI: [10.2139/ssrn.4073551](https://doi.org/10.2139/ssrn.4073551).
- 52 R. Tang, C. Dai, C. Li, W. Liu, S. Gao and C. Wang, Removal of methylene blue from aqueous solution using agricultural residue walnut shell: equilibrium, kinetic, and thermodynamic studies, *J. Chem.*, 2017, **2017**(1), 8404965, DOI: [10.1155/2017/8404965](https://doi.org/10.1155/2017/8404965).
- 53 R. Tabaraki, A. Nateghi and S. Ahmady-Asbchin, Biosorption of lead(II) ions on Sargassum ilicifolium: Application of response surface methodology, *Int. Biodeterior. Biodegrad.*, 2014, **93**, 145–152.
- 54 Y. S. Ho, Citation review of Lagergren kinetic rate equation on adsorption reactions, *Scientometrics*, 2004, **59**(1), 171–177.
- 55 J. W. Guo, Z. Y. Lin, B. R. Huang, C. H. Lu and J. K. Chen, Antigen detection with thermosensitive hydrophilicity of poly(N-isopropylacrylamide)-grafted poly(vinyl chloride) fibrous mats, *J. Mater. Chem. B*, 2018, **6**(21), 3486–3496.
- 56 H. E. Barden, J. Behnsen, U. Bergmann, M. J. Leng, P. L. Manning, P. J. Withers, R. A. Wogelius and B. E. Dongen, Geochemical evidence of the seasonality, affinity and pigmentation of solenopora jurassica, *PLoS One*, 2015, **10**(9), e0138305, DOI: [10.1371/journal.pone.0138305](https://doi.org/10.1371/journal.pone.0138305).
- 57 K. Artyushkova and J. E. Fulghum, Quantification of PVC-PMMA polymer blend compositions by XPS in the presence of X-ray degradation effects, *Surf. Interface Anal.*, 2001, **31**(5), 352–361.
- 58 Ş. Süzer, Ö. Birer, U. A. Sevil and O. Güven, XPS investigations on conducting polymers, *Turkish J. Chem.*, 1998, **22**(1), 59–65.
- 59 C. Jierong, Y. Jing-Lian and Z. Yun-Ze, Surface modification of medical PVC by remote oxygen plasma, *Compos. Interfaces*, 2004, **11**(2), 123–130.
- 60 C. Le Guern, P. Baillif, P. Conil and R. Houot, Adsorption of a lignosulphonate polymer onto PVC and PET surfaces: evaluation by XPS, *J. Mater. Sci.*, 2001, **36**(6), 1547–1554.
- 61 T. Saeed, A. Naeem, T. Mahmood, Z. Ahmad, M. Farooq, Farida, I. U. Din and I. W. Khan, Comparative study for removal of cationic dye from aqueous solutions by manganese oxide and manganese oxide composite, *Int. J. Environ. Sci. Technol.*, 2021, **18**(3), 659–672.
- 62 D. T. Hermann, S. Tome, V. O. Shikuku, J. B. Tchuigwa, A. Spieß, C. Janiak, M. A. Etoh and D. D. Joh Dina, Enhanced performance of hydrogen peroxide modified pozzolan-based geopolymer for abatement of methylene blue from aqueous medium, *Silicon*, 2022, **14**(10), 5191–5206.
- 63 P. Janoš, S. Coskun, V. Pilařová and J. Rejnek, Removal of basic (Methylene Blue) and acid (Egacid Orange) dyes from waters by sorption on chemically treated wood shavings, *Bioresour. Technol.*, 2009, **100**(3), 1450–1453.
- 64 P. S. Kumar, R. Gayathri, C. Senthamarai, M. Priyadharshini, P. S. A. Fernando, R. Srinath and V. V. Kumar, Kinetics, mechanism, isotherm and thermodynamic analysis of adsorption of cadmium ions by surface-modified Strychnos potatorum seeds, *Korean J. Chem. Eng.*, 2012, **29**(12), 1752–1760.



- 65 G. McKay, M. S. Otterburn and J. A. Aga, Fuller's earth and fired clay as adsorbents for dyestuffs – Equilibrium and rate studies, *Water, Air, Soil Pollut.*, 1985, **24**(3), 307–322.
- 66 N. Kannan and M. M. Sundaram, Kinetics and mechanism of removal of methylene blue by adsorption on various carbons – A comparative study, *Dyes Pigm.*, 2001, **51**(1), 25–40.
- 67 M. Uysal and I. Ar, Removal of Cr(vi) from industrial wastewaters by adsorption. Part I: determination of optimum conditions, *J. Hazard. Mater.*, 2007, **149**(2), 482–491.
- 68 S. M. Al-Mashaikhi, E.-S. I. EL-Shafey, S. Al-Busafi and F. O. Suliman, Adsorption of Methylene blue onto hydrophobic activated carbon, *Sultan Qaboos Univ. J. Sci.*, 2023, **28**(1), 42–52.
- 69 V. K. Garg, M. Amita, R. Kumar and R. Gupta, Basic dye (methylene blue) removal from simulated wastewater by adsorption using Indian Rosewood sawdust: a timber industry waste, *Dyes Pigm.*, 2004, **63**(3), 243–250.
- 70 P. Senthil Kumar, S. Ramalingam, C. Senthamarai, M. Niranjanaa, P. Vijayalakshmi and S. Sivanesan, Adsorption of dye from aqueous solution by cashew nut shell: studies on equilibrium isotherm, kinetics and thermodynamics of interactions, *Desalination*, 2010, **261**(1–2), 52–60.
- 71 C. Y. Kuo, C. H. Wu and J. Y. Wu, Adsorption of direct dyes from aqueous solutions by carbon nanotubes: Determination of equilibrium, kinetics and thermodynamics parameters, *J. Colloid Interface Sci.*, 2008, **327**(2), 308–315.
- 72 A. M. Aljeboree, S. J. Baqir and A. F. Alkaim, Experimental studies of thermodynamics parameters: as a model adsorption and removal of textile, *J. Phys.: Conf. Ser.*, 2020, **1664**(1), 012099, DOI: [10.1088/1742-6596/1664/1/012099](https://doi.org/10.1088/1742-6596/1664/1/012099).
- 73 S. Gul, M. Kanwal, R. A. Qazi, H. Gul, R. Khattak, M. S. Khan, F. Khitab and A. E. Krauklis, Efficient Removal of Methyl Red Dye by Using Bark of Hopbush, *Water*, 2022, **14**(18), 2831, DOI: [10.3390/w14182831](https://doi.org/10.3390/w14182831).

